

# Embedding the Zee–Wolfenstein Neutrino Mass Matrix in an $SO(10) \times A_4$ GUT Scenario

Walter Grimus\* and Helmut Kühböck§

Fakultät für Physik, Universität Wien  
Boltzmannngasse 5, A–1090 Wien, Austria

January 22, 2008

## Abstract

We consider renormalizable  $SO(10)$  Yukawa interactions and put the three fermionic 16-plets into the 3-dimensional irreducible  $A_4$  representation. Scanning the possible  $A_4$  representation assignments to the scalars, we find a unique case which allows to accommodate the down-quark and charged-lepton masses. Assuming type II seesaw dominance, we obtain a viable scenario with the Zee–Wolfenstein neutrino mass matrix, i.e., the Majorana mass matrix with a vanishing diagonal. Contributions from the charged-lepton mass matrix resolve the well-known problems with lepton mixing arising from the vanishing diagonal. In our scenario, fermion masses and mixings are well reproduced for both normal and inverted neutrino mass spectra, and  $b$ – $\tau$  Yukawa unification and definite predictions for the effective mass in neutrinoless double- $\beta$  decay are obtained.

---

\*E-mail: walter.grimus@univie.ac.at

§E-mail: helmut.kuehboeck@gmx.at

# 1 Introduction

Grand Unified Theories (GUTs) based on the gauge group  $SO(10)$  [1] are a framework for attempts to understand the observed fermion masses and mixings. These theories feature a 16-dimensional irreducible representation (irrep), the spinor representation, which naturally accommodates all chiral fermions of one Standard Model (SM) generation plus a right-handed neutrino. Furthermore,  $SO(10)$  GUTs allow for type I [2] and type II [3] seesaw mechanisms (see also [4]) for explaining the smallness of the light neutrino masses.

By employing only one scalar in the  $\mathbf{10}$  and one in the  $\overline{\mathbf{126}}$  irrep of  $SO(10)$  in renormalizable Yukawa couplings, the so-called “Minimal Supersymmetric  $SO(10)$  GUT” (MSGUT) [5] has been successful in accounting for all fermion masses and mixings, if one focuses solely on its fermion mass matrices. Moreover, this model has built-in the gauge-coupling unification of the Minimal Supersymmetric Standard Model (MSSM). In-depth studies of the MSGUT have been performed [6, 7], also with inclusion of small [8] and prominent [9] effects of the  $\mathbf{120}$  irrep. Despite its success in reproducing the known fermion masses and mixings, it should be stressed, however, that the MSGUT considered as a whole is too constrained, as its scalar sector does not admit the vacuum expectation values (VEVs) required for the fit in the fermionic sector—see [10] and [7].

However, one is not really satisfied by just reproducing known fermion masses and mixings, one would also like to explain, for instance, the threefold replication of fermion generations, or the peculiar mixing properties of the lepton sector [11], that is, maximal atmospheric and large but non-maximal solar mixing and a small mixing angle  $\theta_{13}$ .  $SO(10)$  models have not yet been successful in explaining such features, but one may try to meet such challenges by considering the possibility of an underlying flavor symmetry group  $G$ . In GUT models based on the product group  $SO(10) \times G$ , the three known fermion generations can be assigned to representations of the flavor group  $G$ . Our choice of  $G$  is guided by the following considerations. Since all irreps of abelian groups are one-dimensional, only non-abelian groups are suited to explain the existence of more than one fermion generation. Furthermore, unlike continuous symmetries, the break-down of discrete global symmetries does, in general, not give rise to undesired Goldstone bosons. This suggests to stick to non-abelian, discrete flavor groups. Only a few  $SO(10) \times G$  models, with  $G$  being non-abelian and discrete, have been studied so far. For instance, models with  $SO(10) \times S_4$  [12] and  $SO(10) \times A_4$  [13] symmetries have already been investigated. In particular, models employing an  $A_4$  [14, 15] flavor symmetry may give tri-bimaximal leptonic mixing [16], but, in general, in such models right- and left-handed fermion fields transform differently under  $A_4$ . However, in  $SO(10)$  GUTs right- and left-handed fermion fields have to transform in the same way under  $A_4$  [17], since there all chiral matter fields of one generation belong to the same  $SO(10)$  irrep. In [13] a non-supersymmetric  $SO(10) \times A_4$  model with type I seesaw dominance has been analyzed, which successfully preserves tri-bimaximal leptonic mixing and can accommodate all known fermion masses. The quark mixing angles, however, are assumed to be zero.

In this paper, we investigate the fermionic sector of renormalizable  $SO(10) \times A_4$  GUT scenarios, with the three fermion families in the three-dimensional irrep of  $A_4$ , while for the  $SO(10)$  scalar irreps occurring in Yukawa couplings we allow all possible  $A_4$  irreps. We do not discuss the difficult problem of vacuum alignment, but rather assume that we

can dispose of the VEVs according to our needs. With this assumption, we will see that the  $SO(10) \times A_4$  structure enforces the building blocks of the fermion mass matrices to consist of diagonal and off-diagonal matrices. A crucial role will play the mass matrices of the down quarks and the charged leptons. Requiring solely that the scenario is able to reproduce down-quark masses and charged-lepton masses, singles out a unique case with respect to the transformation of the scalars under  $SO(10) \times A_4$ . In that unique viable scenario, under the assumption of type II seesaw dominance, we will find the Zee–Wolfenstein form [18, 19] of the mass matrix of light neutrinos. The well-known phenomenological problems [20] of this mass matrix turn out to be completely resolvable by contributions to lepton mixing from the charged-lepton sector. We want to stress, however, that our usage of the  $A_4$  flavor symmetry does *not* enforce tri-bimaximal mixing in the lepton sector.

Though we have in mind a supersymmetrized scenario, supersymmetry enters our considerations only via the fermion masses. For the numerics we use masses at the GUT scale, which have been obtained through the renormalization group equations of the MSSM.

Our paper is organized as follows. In Section 2 we summarize the properties of the Zee–Wolfenstein neutrino mass matrix. The  $SO(10) \times A_4$  GUT scenario is developed in Section 3. The methods and results of our numerical analysis are discussed in Section 4. Section 5 is devoted to the conclusions.

## 2 The Zee–Wolfenstein mass matrix in a nutshell

The Zee model generates Majorana neutrino masses at the one-loop level [18, 21]. Its neutrino mass matrix has, in general, non-zero elements on the diagonal. However, with a suitable  $\mathbb{Z}_2$  symmetry one can enforce a vanishing diagonal in  $\mathcal{M}_\nu$  at the one-loop level [19]. This Zee–Wolfenstein neutrino mass matrix is a symmetric  $3 \times 3$  matrix whose diagonal elements are zero:

$$\mathcal{M}_\nu = \begin{pmatrix} 0 & a & b \\ a & 0 & c \\ b & c & 0 \end{pmatrix}. \quad (1)$$

From now on we will discuss only this case. The restricted Zee model has the property that one can make a basis transformation such that the charged-lepton mass matrix is diagonal but the form of  $\mathcal{M}_\nu$  given by (1) persists. Thus, without loss of generality, we will assume in this section that the charged-lepton mass matrix is diagonal.

In diagonalizing the matrix (1), one can first remove the phases of  $\mathcal{M}_\nu$ . These phases can be absorbed into the charged-lepton fields. Thus we take the matrix entries  $a, b, c$  to be real. Since the Zee–Wolfenstein mass matrix is traceless and symmetric one has [22]

$$\lambda_1 + \lambda_2 + \lambda_3 = 0, \quad (2)$$

where the  $\lambda_i$  denote the real eigenvalues of  $\mathcal{M}_\nu$ . Writing  $m_i$  for the masses of the light neutrinos, we have  $m_i = |\lambda_i|$ .

In the case of inverted ordering  $m_3 < m_1 < m_2$  of the neutrino masses ( $\Delta m_\odot^2 = m_2^2 - m_1^2$ ,  $\Delta m_{\text{atm}}^2 = m_2^2 - m_3^2$ ), it has been pointed out in Ref. [20] that the mass matrix (1) together with  $\Delta m_\odot^2 \ll \Delta m_{\text{atm}}^2$  leads, for all practical purposes, to maximal solar mixing

$\theta_{12} = \pi/4$  and  $\theta_{13} = 0$ . Furthermore, the atmospheric mixing angle  $\theta_{23}$  can be *chosen* to be maximal. While the latter two properties are most welcome, maximal solar mixing is excluded by more than  $5\sigma$  by experimental data [23]. In [24] it has been shown that deviations from maximal solar mixing are severely constrained through

$$|\cos 2\theta_{12}| \lesssim \frac{1}{4} \frac{\Delta m_{\odot}^2}{\Delta m_{\text{atm}}^2}. \quad (3)$$

The neutrino masses are approximately given by

$$m_3 \simeq \frac{1}{2} \frac{\Delta m_{\odot}^2}{\sqrt{\Delta m_{\text{atm}}^2}}, \quad m_1 \simeq m_2 \simeq \sqrt{\Delta m_{\text{atm}}^2}. \quad (4)$$

Thus one obtains  $m_3 \ll m_1 \simeq m_2$  and the resulting neutrino mass spectrum exhibits an inverted hierarchy.

In the case of the normal ordering  $m_1 < m_2 < m_3$  of the neutrino masses ( $\Delta m_{\odot}^2 = m_2^2 - m_1^2$ ,  $\Delta m_{\text{atm}}^2 = m_3^2 - m_1^2$ ) things are even worse. Although it is now possible to have maximal atmospheric mixing and, at the same time, allowing the solar mixing angle to be in perfect agreement with experimental data, the mixing angle  $\theta_{13}$  turns out to be much too large [20]:

$$\sin^2 \theta_{13} \simeq \frac{1}{3}. \quad (5)$$

The neutrino mass spectrum can be estimated by

$$m_1 \simeq m_2 \simeq \frac{1}{2} m_3 \simeq \sqrt{\frac{\Delta m_{\text{atm}}^2}{3}}. \quad (6)$$

Therefore, all neutrino masses will be of the same order of magnitude, but the mass spectrum cannot be quasi-degenerate.

Concerning neutrinoless double- $\beta$  decay, the relevant observable is the effective Majorana neutrino mass  $|\langle m_{\beta\beta} \rangle| \equiv |\sum_i U_{ei}^2 m_i|$ , where  $U$  denotes the unitary leptonic mixing (PMNS) matrix. The mass  $|\langle m_{\beta\beta} \rangle|$  is equal to the modulus of the  $(e, e)$  matrix element of  $\mathcal{M}_{\nu}$ , which is exactly zero in the Zee–Wolfenstein case. Thus the model prevents neutrinoless double- $\beta$  decay.

In summary, the Zee–Wolfenstein model is not viable because it does not give a consistent explanation of *all* current experimental data of the neutrino sector (*i.e.* two mass-squared differences plus three mixings angles). It is the purpose of this paper to embed the Zee–Wolfenstein neutrino mass matrix in an  $SO(10)$  GUT. In such an environment, the zeros in the diagonal of  $\mathcal{M}_{\nu}$  are *not* stable under a basis change such that the charged-lepton mass matrix becomes diagonal. Therefore, as we will show, contributions from the charged-lepton sector can provide the necessary remedy for correcting the too large mixing angle  $\theta_{12}$  in the case of inverted hierarchy and  $\theta_{13}$  in the case of normal hierarchy [25]. As an additional bonus, a non-vanishing  $|\langle m_{\beta\beta} \rangle|$  and, therefore, neutrinoless double- $\beta$  decay becomes possible.

### 3 The $SO(10) \times A_4$ model

The tensor product of the  $SO(10)$  spinor representation of the fermions is given by [26, 27]

$$\mathbf{16} \otimes \mathbf{16} = (\mathbf{10} \oplus \mathbf{126})_S \oplus \mathbf{120}_{AS}, \quad (7)$$

where the subscripts S and AS refer to symmetric and antisymmetric Yukawa coupling matrices, respectively. Renormalizable  $SO(10)$  GUTs can generate fermion masses at the tree level only by the scalar irreps  $\mathbf{10}$ ,  $\mathbf{120}$  and  $\overline{\mathbf{126}}$ .

The 12-element group  $A_4$  is popular as a family symmetry in model building— see [14] for a selection of the vast  $A_4$  literature and [15] for a review on the group  $A_4$  and models. It has three one-dimensional irreps and one three-dimensional irrep. The tensor product  $\mathbf{3} \otimes \mathbf{3}$  contains all one-dimensional irreps exactly once, but the three-dimensional irrep is contained twice. While the Yukawa couplings corresponding to the one-dimensional irreps are diagonal and, therefore, symmetric, the couplings of the  $\mathbf{3} \oplus \mathbf{3} \in \mathbf{3} \otimes \mathbf{3}$  are off-diagonal, but no special symmetry property is fixed. However, Eq. (7) suggests to choose one three-dimensional irrep with symmetric and the other one with antisymmetric tensor indices:

$$\mathbf{3} \otimes \mathbf{3} = (\mathbf{1} \oplus \mathbf{1}' \oplus \mathbf{1}'' \oplus \mathbf{3})_S \oplus \mathbf{3}_{AS}. \quad (8)$$

Now we consider  $SO(10) \times A_4$  and investigate possible Yukawa couplings and fermion mass matrices under the assumption that the fermions transform as  $\mathbf{16} \otimes \mathbf{3}$ , which is clearly the only reasonable choice if we want to take advantage of the non-abelian character of  $A_4$ . Equations (7) and (8) dictate that the  $\mathbf{120}$  can only transform as a  $\mathbf{3}$  under  $A_4$ , while for the  $\mathbf{10}$  and  $\overline{\mathbf{126}}$  singlet *and* triplet irreps of  $A_4$  are possible. Let us consider the case where the scalars responsible for Yukawa couplings transform as

$$\mathbf{10} \otimes (\mathbf{1} \oplus \mathbf{1}' \oplus \mathbf{1}'') \quad \text{and} \quad \overline{\mathbf{126}} \otimes \mathbf{3}. \quad (9)$$

Then, in a symbolic way, writing down only the  $A_4$  part, the Yukawa couplings are given by

$$\sum_{i=1}^3 h_i \sum_{a=1}^3 \omega^{(i-1)(a-1)} \mathbf{16}_a \mathbf{16}_a \mathbf{10}_i + \quad (10)$$

$$(\mathbf{16}_2 \mathbf{16}_3 + \mathbf{16}_3 \mathbf{16}_2) \overline{\mathbf{126}}_1 + (\mathbf{16}_3 \mathbf{16}_1 + \mathbf{16}_1 \mathbf{16}_3) \overline{\mathbf{126}}_2 + (\mathbf{16}_1 \mathbf{16}_2 + \mathbf{16}_2 \mathbf{16}_1) \overline{\mathbf{126}}_3, \quad (11)$$

where  $a$  is a family index and  $\omega = (-1 + i\sqrt{3})/2$ . Furthermore, we make two assumptions:

- i) All VEVs which occur in the scalars can have independent values.
- ii) Type II seesaw dominates in the neutrino mass matrix.

These assumptions together with Eq. (9) define the scenario we will investigate in the following.

We furthermore assume that our models can be extended in a suitable way to solve the doublet-triplet splitting problem.<sup>1</sup> Moreover, since we have in mind the MSSM, with only

---

<sup>1</sup>For instance, the Dimopoulos–Wilczek mechanism [29] and the missing partner mechanism [30] provide viable solutions of the doublet-triplet splitting problem in  $SO(10)$  GUTs.

two Higgs doublets, as the low-energy limit of our  $SO(10)$  models we must assume a suitable doublet-doublet splitting as well, which is usually achieved by finetuning [31]. These assumptions are not innate to the models presented here but are well-known problems in GUTs.

Let us now derive some consequences of our scenario. Because of assumption i), the Yukawa couplings (10) produce *diagonal* mass terms with three independent entries, one for the up-quark mass matrix ( $q = u$ ) and another one for the down quark mass matrix ( $q = d$ ):

$$\text{diag} (h_1 v_{q1} + h_2 v_{q2} + h_3 v_{q3}, h_1 v_{q1} + \omega h_2 v_{q2} + \omega^2 h_3 v_{q3}, h_1 v_{q1} + \omega^2 h_2 v_{q2} + \omega h_3 v_{q3}), \quad (12)$$

where the  $v_{qi}$  are the VEVs appearing in the scalar 10-plets. Next we consider the Yukawa couplings (11). Again because of assumption i), this Yukawa interaction generates two independent *off-diagonal* contributions to the mass matrices of up and down quarks.

Studying the system of mass matrices, we find that assumptions i) and ii) lead to a decoupling of the up-quark mass matrix  $M_u$  from the rest of the system. This is so because the quark mass matrices are given by  $M_u = H' + F'$  and  $M_d = H + F$ , where  $H'$  and  $H$  are independent diagonal matrices, while  $F'$  and  $F$  are independent off-diagonal matrices. Therefore,  $M_u$  would only be related to the system of mass matrices through the neutrino Dirac-mass matrix  $M_D = H' - 3F'$ , but this relationship is irrelevant due to assumption ii). Since  $M_u$  is a general symmetric matrix independent of the rest of the system of mass matrices, the CKM matrix can always be reproduced. The other side of the coin is that our scenario loses predictivity because it is neither restricted by the values of the up-quark masses nor by the experimental information on the CKM matrix.

The remaining system of mass matrices which we want to study consists of the mass matrices of down-type quarks and charged-leptons, given by

$$M_d = H + F \quad \text{and} \quad M_\ell = H - 3F, \quad (13)$$

respectively, where  $H$  is diagonal, while  $F$  is off-diagonal, and of the neutrino mass matrix  $\mathcal{M}_\nu$  of Eq. (1). Without loss of generality,  $H$  can be assumed to be real, but  $F$  and  $\mathcal{M}_\nu$  have complex entries.<sup>2</sup> Note that in view of assumption i) the entries in  $\mathcal{M}_\nu$  are independent of  $F$ , but  $M_\ell$  and  $\mathcal{M}_\nu$  are coupled via the PMNS matrix

$$U = U_\ell^\dagger U_\nu \quad \text{with} \quad U_\ell^T M_\ell U_\ell = \text{diag} (m_e, m_\mu, m_\tau), \quad U_\nu^T \mathcal{M}_\nu U_\nu = \text{diag} (m_1, m_2, m_3). \quad (14)$$

Counting the number of parameters, we find nine absolute values and five phases,<sup>3</sup> while the number of observables to be fitted is 11: three charged-lepton masses, three down-quark masses, two neutrino mass-squared differences and three lepton mixing angles. The fitting procedure and predictions of our scenario will be exposed in the next section.

We note that the family symmetry  $A_4$  has the effect of generating independent diagonal and off-diagonal contributions to the quark and lepton mass matrices. Adhering to the two assumptions presented above but using other  $A_4$  representations than those of Eq. (9), we can find several other scenarios. E.g., with 120-plets, antisymmetric off-diagonal mass

---

<sup>2</sup>Now we cannot absorb the phases of  $\mathcal{M}_\nu$  into the charged-lepton fields since  $M_\ell$  is not diagonal.

<sup>3</sup>Of the three phases in  $\mathcal{M}_\nu$  one can be removed.

Leptons		Quarks	
$m_e$	$0.3585^{+0.0003}_{-0.0003}$	$m_d$	$1.03 \pm 0.41$
$m_\mu$	$75.6715^{+0.0578}_{-0.0501}$	$m_s$	$19.6 \pm 5.2$
$m_\tau$	$1292.2^{+1.3}_{-1.2}$	$m_b$	$1063.6^{+141.4}_{-086.5}$
$\Delta m_\odot^2$	$(7.9 \pm 0.3) \times 10^{-5}$		
$\Delta m_{\text{atm}}^2$	$(2.50^{+0.20}_{-0.25}) \times 10^{-3}$		
$s_{12}^2$	$0.31 \pm 0.025$		
$s_{23}^2$	$0.50 \pm 0.065$		
$s_{13}^2$	$< 0.0155$		

Table 1: Input data (central values and  $1\sigma$  errors) at the GUT scale of  $M_{\text{GUT}} = 2 \times 10^{16}$  GeV for  $\tan\beta = 10$ . The charged-fermion masses are taken from [32], except for the values of  $m_d$  and  $m_s$ ; these were obtained by taking their low-energy values from [33] and scaling them to  $M_{\text{GUT}}$ . As for  $\Delta m_{\text{atm}}^2$ , we use the value obtained in [23]. We have copied the remaining input from Table I in [7]. Charged-fermion masses are in units of MeV, neutrino mass-squared differences in  $\text{eV}^2$ . We have used the abbreviations  $s_{12}^2 \equiv \sin^2\theta_{12}$ , *etc.* The angles in the left table refer to the PMNS matrix.

matrix contributions are generated. A list of such cases is presented in Table 2. There we confine ourselves to a maximum of three scalars per  $SO(10)$  irrep, the 126-plet must always be present to allow a viable type II seesaw neutrino mass matrix and the **10** and **120** are not present at the same time; the latter condition is for avoiding a proliferation of parameters. However, it will turn out that the only viable scenario is the one defined via Eq. (9).

## 4 The numerical analysis

We perform a global  $\chi^2$  analysis of the  $SO(10) \times A_4$  scenario defined by Eq. (9) and assumptions i) and ii) by employing the downhill simplex method [28]. In Table 1 the observable quantities  $O_i$  are specified in the form

$$O_i = \bar{O}_i \pm \sigma_i, \quad (15)$$

where  $\bar{O}_i$  and  $\sigma_i$  denote central values and  $1\sigma$  deviations, respectively. The index  $i = 1, \dots, 11$  labels the different observables given in Table 1. The masses in that table refer to the mass values at a GUT scale of  $2 \times 10^{16}$  GeV, obtained via the renormalization group equations of the MSSM, for the ratio of Higgs doublet VEVs  $\tan\beta = 10$ .<sup>4</sup> Writing

<sup>4</sup>Since we do not have quasi-degenerate neutrino mass spectra, the effect of the renormalization group running on the lepton mixing angles is negligible [34].

Model	<b>10</b>	<b>120</b>	$\overline{\mathbf{126}}$	$\chi_{d\ell}^2$
A	<b>3</b>	–	<b>3</b>	$10^6$
B	–	<b>3</b>	<b>3</b>	46
C	<b>3</b>	–	$\mathbf{1} \oplus \mathbf{1}' \oplus \mathbf{1}''$	46
D	–	<b>3</b>	$\mathbf{1} \oplus \mathbf{1}' \oplus \mathbf{1}''$	46
E'	<b>1</b>	–	<b>3</b>	$7 \times 10^4$
E	$\mathbf{1} \oplus \mathbf{1}' \oplus \mathbf{1}''$	–	<b>3</b>	0.89

Table 2: A variety of renormalizable GUT models based on  $SO(10) \times A_4$ . Each line corresponds to a distinctive model scenario. Columns 2–4 specify the transformation properties of the  $SO(10)$  scalar multiplets under the flavor symmetry group  $A_4$ . The last column gives the best-fit values  $\chi_{d\ell}^2$  when fitting charged-lepton and down-type quark masses.

$\mathbf{x}$  for the set the 14 model parameters and  $P_i(\mathbf{x})$  for the resulting model predictions, one can define a  $\chi^2$  function by

$$\chi^2(\mathbf{x}) = \sum_{i=1}^{11} \left( \frac{P_i(\mathbf{x}) - \bar{O}_i}{\sigma_i} \right)^2. \quad (16)$$

The global minimum of  $\chi^2$  will represent the best possible agreement of theoretical predictions and experimental data. This minimization task is performed using the downhill simplex method.

For investigating the variation of  $\chi^2$  as a function of the value  $\widehat{O}$  of an observable  $O$ , we add the “pinning term”  $(P(\mathbf{x}) - \widehat{O})^2 / (0.01 \widehat{O})^2$  to  $\chi^2$ , where  $P(\mathbf{x})$  represents the theoretical prediction for  $O$ . Note that if  $O$  agrees with one of observables  $O_i$  occurring in  $\chi^2$  of Eq. (16), the  $O_i$  term has to be removed from Eq. (16). The small error in the denominator of the “pinning term” guarantees to pin the observable  $O$  down to the value  $\widehat{O}$ . The pinning procedure performs as desired when the contribution of the pinning term to  $\chi^2$  is negligible.

As mentioned at the end of Section 3, we have not only investigated the scenario defined by Eq. (9) but also a variety of others which are characterized by the  $A_4$  transformation properties of their scalar  $SO(10)$  multiplets in columns 2–4 of Table 2 (models A–E'). We have found that all these scenarios fail already to reproduce the down-quark and charged-lepton masses—see the value of the corresponding  $\chi_{d\ell}^2$  in the last column of Table 2.<sup>5</sup> For comparison we have also presented the  $\chi_{d\ell}^2$  of our successful scenario in the line labeled by E, which will be investigated in the rest of this paper.

---

<sup>5</sup>For case A this failure is trivial:  $M_d$  and  $M_\ell$  are symmetric with a vanishing diagonal, therefore, Eq. (2) holds, which is in contradiction to the strong hierarchy in the down-quark and charged-lepton masses.



## 4.1 Predictions for the case of normal neutrino mass ordering

We search for the best-fit solution for the normal neutrino mass spectrum  $m_1 < m_2 < m_3$ . In this case we find an excellent fit with the following properties:

$$\begin{aligned} \chi^2 &= 0.96, \\ m_1 &= 2.795 \times 10^{-2} \text{ eV}, \quad m_2 = 2.933 \times 10^{-2} \text{ eV}, \quad m_3 = 5.728 \times 10^{-2} \text{ eV}. \end{aligned} \quad (17)$$

The corresponding values of the matrix elements of  $H$ ,  $F$ ,  $\mathcal{M}_\nu$  are given by

$$\begin{aligned} H &= \begin{pmatrix} 14.8905 & 0 & 0 \\ 0 & 14.9798 & 0 \\ 0 & 0 & 1189.49 \end{pmatrix}, \\ F &= \begin{pmatrix} 0 & 4.45699 e^{i0.990889\pi} & 83.3159 e^{-i0.940907\pi} \\ 4.45699 e^{i0.990889\pi} & 0 & 86.5511 e^{i0.946557\pi} \\ 83.3159 e^{-i0.940907\pi} & 86.5511 e^{i0.946557\pi} & 0 \end{pmatrix}, \\ \mathcal{M}_\nu &= \begin{pmatrix} 0 & 2.83435 e^{i0.267950\pi} & 2.93292 e^{i0.649567\pi} \\ 2.83435 e^{i0.267950\pi} & 0 & 2.82486 e^{i0.5\pi} \\ 2.93292 e^{i0.649567\pi} & 2.82486 e^{i0.5\pi} & 0 \end{pmatrix} \times 10^{-2}, \end{aligned} \quad (18)$$

where the numerical values in  $H$  and  $F$  are in units of MeV, while the entries in  $\mathcal{M}_\nu$  are in units of eV.

The non-zero value of  $\chi^2$  stems from the deviation of the bottom-quark mass  $m_b$  from its central value by  $+0.98\sigma$ . The remaining observables of Table 1 are fitted perfectly. Thus the model succeeds in correcting the too large value for the mixing angle  $\theta_{13}$  of the Zee–Wolfenstein model, despite the close relationship between  $M_d$  and  $M_\ell$  given by Eq. (13) which, on the other hand, leads to the desired unification of  $m_b$  and  $m_\tau$ , as will be discussed in Section 4.3.

As explained in Section 2, the three light neutrino masses cannot be independent of each other. The sum of the eigenvalues of  $\mathcal{M}_\nu$  must be zero, which translates into  $m_1 + m_2 - m_3 = 0$ . This can easily be verified for the neutrino masses of the best-fit (17). The sum of the neutrino masses is  $\Sigma \equiv \sum_i m_i = 2 m_3 = 0.11 \text{ eV}$ , which lies safely below the cosmological bound  $\Sigma \lesssim 1 \text{ eV}$  [35].

The neutrino mass spectrum has to fulfill the approximate relation (6). Inserting the central value for  $\Delta m_{\text{atm}}^2$  from Table 1 into Eq. (6) gives  $m_1 \simeq m_2 \simeq 2.89 \times 10^{-2} \text{ eV}$  and  $m_3 \simeq 5.77 \times 10^{-2} \text{ eV}$ , which is in good agreement with the above best-fit results.

The quantity  $R \equiv m_1/\sqrt{\Delta m_\odot^2}$  measures how hierarchical a neutrino mass spectrum is.  $\chi^2$  as a function of  $R$  is depicted in the right panel of Figure 1. We read off that  $R \sim 3.1$  is preferred and for the values  $2.4 \lesssim R \lesssim 3.7$  one obtains fits with  $\chi^2 \lesssim 15$ . Thus the mass spectrum is neither hierarchical nor quasi-degenerate,<sup>6</sup> but is located between these extrema. The narrow range of allowed values for  $R$  reflects the clear-cut prediction of the Zee–Wolfenstein mass matrix for the neutrino mass spectrum.

Figure 1 (left panel) shows the constraints on the atmospheric mixing angle  $\theta_{23}$ . One can see that values of  $\sin^2 \theta_{23}$  smaller than 0.38 ( $-2\sigma$ ) are strongly disfavored and thus

---

<sup>6</sup>Typically, quasi-degenerate neutrino spectra would correspond to  $R \gtrsim \sqrt{\Delta m_{\text{atm}}^2/\Delta m_\odot^2} \simeq 5.6$ .

a strict lower bound for  $\theta_{23}$  is established. However, very good fits are also possible for values of  $\sin^2 \theta_{23}$  significantly larger than the best-fit value of 0.5.

Concerning the solar mixing angle, Figure 1 (middle panel) shows that the whole physically allowed range for  $\sin^2 \theta_{12}$  gives excellent fits and therefore no prediction can be obtained.

Regarding the mixing angle  $\theta_{13}$ , the best-fit solution gives a value of  $\sin^2 \theta_{13} = 2 \times 10^{-4}$ . However, also significantly smaller (down to  $10^{-6}$ ) and larger values (up to 0.1) for  $\sin^2 \theta_{13}$  are equally allowed. Thus the severe problem of the original Zee–Wolfenstein mass matrix ( $\sin^2 \theta_{13} \simeq 1/3$ ) can be resolved completely by contributions from the charged-lepton sector.

The best-fit gives  $\delta_{\text{PMNS}} = 31^\circ$  for the leptonic CP phase. However, varying  $\delta_{\text{PMNS}}$  shows that the whole  $[0^\circ, 360^\circ]$  range allows for very good fits and therefore no prediction can be made.

The effective Majorana mass of neutrinoless double- $\beta$  decay  $|\langle m_{\beta\beta} \rangle|$  for the normal spectrum is given by

$$|\langle m_{\beta\beta} \rangle| = \left| \left( m_1 c_{12}^2 + \sqrt{m_1^2 + \Delta m_\odot^2} s_{12}^2 e^{i\beta_1} \right) c_{13}^2 + \sqrt{m_1^2 + \Delta m_{\text{atm}}^2} s_{13}^2 e^{i\beta_2} \right|, \quad (19)$$

where  $\beta_1$  and  $\beta_2$  are Majorana phases. Here and in the following we use the abbreviations  $c_{12} \equiv \cos \theta_{12}$ ,  $s_{12} \equiv \sin \theta_{12}$ , *etc.* After inserting into Eq. (19)  $m_1$  from the best-fit (17), employing for the other parameters the corresponding central values from Table 1, and varying the two phases  $\beta_1$  and  $\beta_2$  *freely* between  $0^\circ$  and  $360^\circ$ , we obtain the bounds

$$10.2 \text{ meV} \leq |\langle m_{\beta\beta} \rangle| \leq 28.4 \text{ meV}. \quad (20)$$

On the other hand, the phases  $\beta_1$  and  $\beta_2$  are actually functions of the parameters of our scenario and are determined by the fit. Using the best-fit parameters (18) for the calculation of the effective Majorana mass, we obtain  $|\langle m_{\beta\beta} \rangle| = 28.4 \text{ meV}$ , which is identical to the upper bound in (20). Figure 2 presents the change of  $\chi^2$  when  $|\langle m_{\beta\beta} \rangle|$  is varied. We can read off that the range for the effective mass is much more restricted than (20) would suggest. Obviously, the increase of  $\chi^2$  for larger values of  $|\langle m_{\beta\beta} \rangle|$  is caused by exceeding the upper bound of (20). The strong increase of  $\chi^2$  for smaller values of  $|\langle m_{\beta\beta} \rangle|$ , however, is a clear-cut model prediction. For instance, allowing for only moderate good fits with  $\chi^2 \lesssim 5$  results in the severely restricted range  $25 \text{ meV} \lesssim |\langle m_{\beta\beta} \rangle| \lesssim 31 \text{ meV}$ , which could be tested by future neutrinoless double- $\beta$  decay experiments sensitive to  $|\langle m_{\beta\beta} \rangle| \gtrsim 10 \text{ meV}$ .

## 4.2 Predictions for the case of inverted neutrino mass ordering

The best-fit solution for the inverted neutrino mass spectrum  $m_3 < m_1 < m_2$  turns out to be excellent as well. It is characterized by the following properties:

$$\begin{aligned} \chi^2 &= 0.92, \\ m_1 &= 4.921 \times 10^{-2} \text{ eV}, \quad m_2 = 5.000 \times 10^{-2} \text{ eV}, \quad m_3 = 7.963 \times 10^{-4} \text{ eV}, \end{aligned} \quad (21)$$

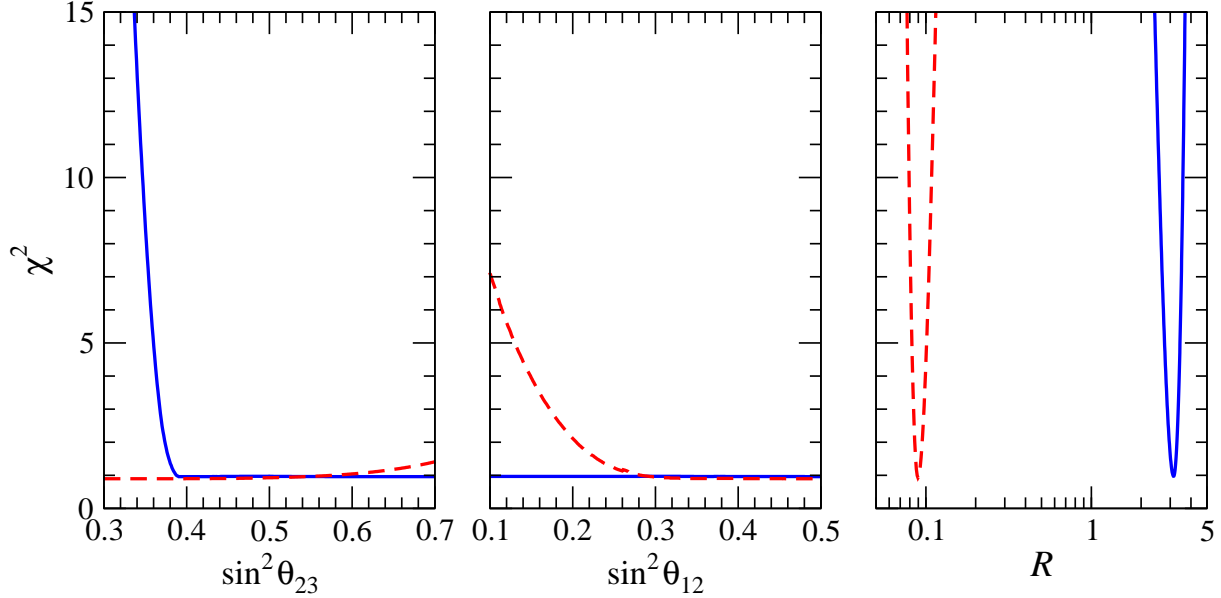


Figure 1:  $\chi^2$  as a function of  $\sin^2 \theta_{23}$  (left panel),  $\sin^2 \theta_{12}$  (middle panel) and of  $R \equiv m_{\min}/\sqrt{\Delta m_{\odot}^2}$  (right panel), where  $m_{\min} = m_1$  for the normal and  $m_3$  for the inverted neutrino mass spectrum. The solid lines correspond to normal neutrino mass ordering, while the dashed lines refer to the inverted neutrino mass spectrum.

with the matrices

$$\begin{aligned}
 H &= \begin{pmatrix} 8.24821 & 0 & 0 \\ 0 & 23.3969 & 0 \\ 0 & 0 & 1184.52 \end{pmatrix}, \\
 F &= \begin{pmatrix} 0 & 6.34572 e^{i\pi} & 39.2455 \\ 6.34572 e^{i\pi} & 0 & 116.271 \\ 39.2455 & 116.271 & 0 \end{pmatrix}, \\
 \mathcal{M}_\nu &= \begin{pmatrix} 0 & 4.32801 & 2.42291 e^{i\pi} \\ 4.32801 & 0 & 0.0934209 e^{i\pi} \\ 2.42291 e^{i\pi} & 0.0934209 e^{i\pi} & 0 \end{pmatrix} \times 10^{-2},
 \end{aligned} \tag{22}$$

where the numerical values in  $H$  and  $F$  are in units of MeV, while the entries in  $\mathcal{M}_\nu$  are in units of eV.

The  $\chi^2$  analysis reveals that the removal of the non-trivial complex phases from  $F$  and  $\mathcal{M}_\nu$  does not affect the goodness of the fit. Thus we specified here the fitting parameters for the CP conserving case.<sup>7</sup> However, the subsequent numerical analysis is performed with the inclusion of the five phase parameters (CP non-conservation). As in the case of normal neutrino mass ordering, the main contribution to  $\chi^2$  is caused by the bottom-quark mass  $m_b$ , being too large by  $0.95\sigma$ . All the other observables are fitted very accurately.

<sup>7</sup>For the normal neutrino spectrum, however, the CP conserving case results in a worse, but still very good fit with  $\chi^2 = 1.94$ . Here, the main contributions to  $\chi^2$  stem from  $m_b$  ( $+1.23\sigma$ ) and  $\sin^2 \theta_{23}$  ( $-0.64\sigma$ ).

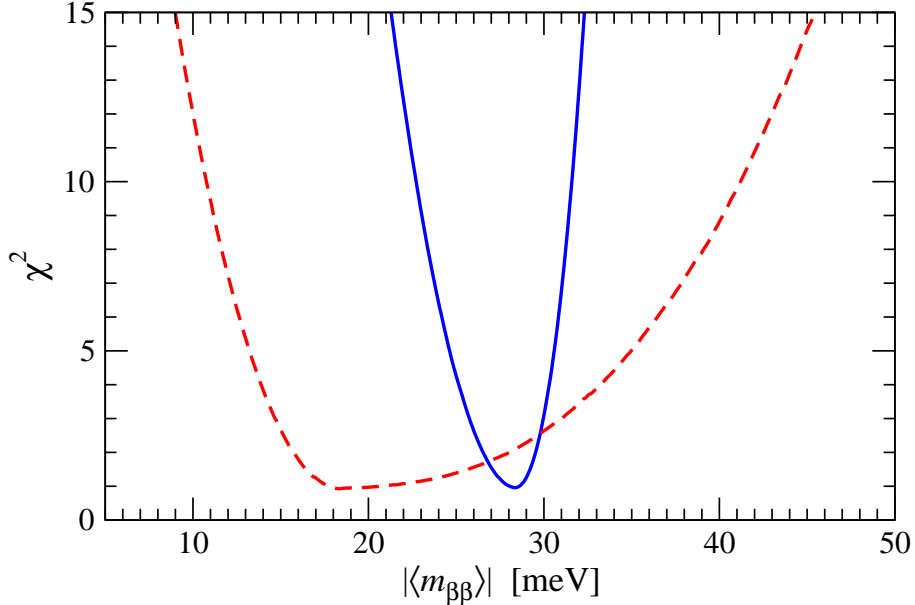


Figure 2:  $\chi^2$  as a function of the effective Majorana mass  $|\langle m_{\beta\beta} \rangle|$  probed in neutrinoless double- $\beta$  decay experiments. The solid line corresponds to normal neutrino mass ordering, while the dashed line refers to the inverted neutrino mass spectrum.

Thus the GUT model allows for a considerably reduction of the maximal solar mixing angle  $\theta_{12}$ , which spoiled the Zee–Wolfenstein model.

$\mathcal{M}_\nu$  being of the Zee–Wolfenstein form implies  $m_1 - m_2 + m_3 = 0$  for the three light neutrino masses. Taking the neutrino masses from the best-fit (21), we get  $\Sigma \equiv \sum_i m_i = 2m_2 = 0.10$  eV, which is safely below the cosmological limit [35]. Inserting the central values for the mass-squared differences from Table 1 into Eqs. (4) gives  $m_1 \simeq m_2 \simeq 5 \times 10^{-2}$  eV and  $m_3 \simeq 7.9 \times 10^{-4}$  eV, which is in good agreement with the numerically obtained best-fit values (21).

$\chi^2$  as a function of  $R \equiv m_3/\sqrt{\Delta m_{21}^2}$  is shown in Figure 1 (right panel). We can read off that  $R \sim 0.09$  is preferred and for the values  $0.077 \lesssim R \lesssim 0.11$  one gets fits with  $\chi^2 \lesssim 15$ . As in the case of normal neutrino mass ordering, the range for  $R$  is very restricted. Hierarchy is strongly preferred, however, too small values for  $m_3$  are strictly forbidden.

Figure 1 (middle panel) depicts the constraints on the solar mixing angle  $\theta_{12}$ . We can read off that values for  $\sin^2 \theta_{12}$  smaller than 0.3 become increasingly disfavored. However, very good fits can also be found for values of  $\sin^2 \theta_{12}$  larger than the best-fit value, and maximal solar mixing also represents a very good fit.

Regarding the atmospheric mixing angle  $\theta_{23}$ , Figure 1 (left panel) reveals that the whole physically allowed range for  $\sin^2 \theta_{23}$  gives very good fits and therefore no prediction can be obtained. This property is seemingly a legacy of the original Zee–Wolfenstein model, where the atmospheric mixing angle for inverted neutrino mass ordering is unconstrained [20].

As for the mixing angle  $\theta_{13}$ , we find  $\sin^2 \theta_{13} = 2.5 \times 10^{-3}$  for the best fit. However,

pinning  $\sin^2 \theta_{13}$  in  $\chi^2$  shows that also smaller (down to  $10^{-6}$ ) and larger values (up to 0.1) are possible. For instance, enforcing  $\sin^2 \theta_{13} = 10^{-6}$  still allows  $\chi^2 = 3.1$ .

Concerning the leptonic CP phase  $\delta_{\text{PMNS}}$ , the specified best-fit, which employs only trivial complex phases, gives  $\delta_{\text{PMNS}} = 180^\circ$ . However, varying  $\delta_{\text{PMNS}}$  in the range  $(90^\circ, 270^\circ)$  allows for fits of equally good quality. Only the neighborhood of  $\delta_{\text{PMNS}} \simeq 0^\circ$  seems to be slightly disfavored by  $\chi^2 \simeq 3.2$ .

The effective Majorana mass for the neutrinoless double- $\beta$  decay is given by

$$|\langle m_{\beta\beta} \rangle| = \left| \left( \sqrt{m_3^2 + \Delta m_{\text{atm}}^2 - \Delta m_\odot^2} c_{12}^2 e^{i\beta_1} + \sqrt{m_3^2 + \Delta m_{\text{atm}}^2} s_{12}^2 e^{i\beta_2} \right) c_{13}^2 + m_3 s_{13}^2 \right|. \quad (23)$$

With  $m_3$  from the best-fit and taking for the other parameters in (23) the corresponding central values in Table 1, free variation of the two complex phases results in the following bounds on the effective Majorana neutrino mass:

$$18.5 \text{ meV} \leq |\langle m_{\beta\beta} \rangle| \leq 49.5 \text{ meV}. \quad (24)$$

On the other hand, employing the best-fit parameters (22), we obtain  $|\langle m_{\beta\beta} \rangle| = 18.4 \text{ meV}$ , which is located close to the lower bound of (24).

Figure 2 shows the change of  $\chi^2$  under variations of  $|\langle m_{\beta\beta} \rangle|$ . We can see that the range for the effective mass is less restricted than in the case of normal neutrino spectrum. Clearly, the strong increase of  $\chi^2$  for smaller values of  $|\langle m_{\beta\beta} \rangle|$  comes from falling below the lower bound of (24). The rise of  $\chi^2$  is less dramatic when moving to larger values of  $|\langle m_{\beta\beta} \rangle|$ . However, there is a clear bias towards values of  $|\langle m_{\beta\beta} \rangle|$  in the lower half of the range spanned by (24). We can also read off from Figure 2 that allowing moderately good fits with  $\chi^2 \lesssim 5$  gives  $13 \text{ meV} \lesssim |\langle m_{\beta\beta} \rangle| \lesssim 35 \text{ meV}$ . Moreover, we can see that the  $|\langle m_{\beta\beta} \rangle|$  regions where  $\chi^2 \gtrsim 2$  are overlapping for both neutrino mass orderings and thus one cannot discriminate with  $|\langle m_{\beta\beta} \rangle|$  between normal and inverted mass spectrum in the overlap region. However,  $|\langle m_{\beta\beta} \rangle| \lesssim 20 \text{ meV}$  (which is preferred) or  $|\langle m_{\beta\beta} \rangle| \gtrsim 33 \text{ meV}$  is only possible for an inverted hierarchy in our scenario.

### 4.3 $b - \tau$ unification

As has already been noticed in Sections 4.1 and 4.2, both best-fit values of  $m_b$  are located near the upper  $1\sigma$  bound of its input value from Table 1. The ratio  $m_b/m_\tau$ , using the mean values from Table 1, is 0.82. Employing the best-fit values for  $m_b$  and  $m_\tau$ , this ratio is higher, namely  $m_b/m_\tau = 0.93$  for both normal and inverted neutrino mass ordering.

Figure 3 depicts  $\chi^2$  as a function of  $m_b$  for both neutrino mass orderings. This figure clearly reflects the feature mentioned above since for values of  $m_b$  below 1190 MeV,  $\chi^2$  increases dramatically and lower values of  $m_b$  become strictly ruled out.

There also exists an upper bound on  $m_b$  in Figure 3 at about 1250 MeV, which is located *below* the central input value of  $m_\tau$  at 1292 MeV. In contrast to the normal neutrino mass spectrum, however, the inverted spectrum seems to prefer values for  $m_b$  near its lower bound, as can be read off from Figure 3.

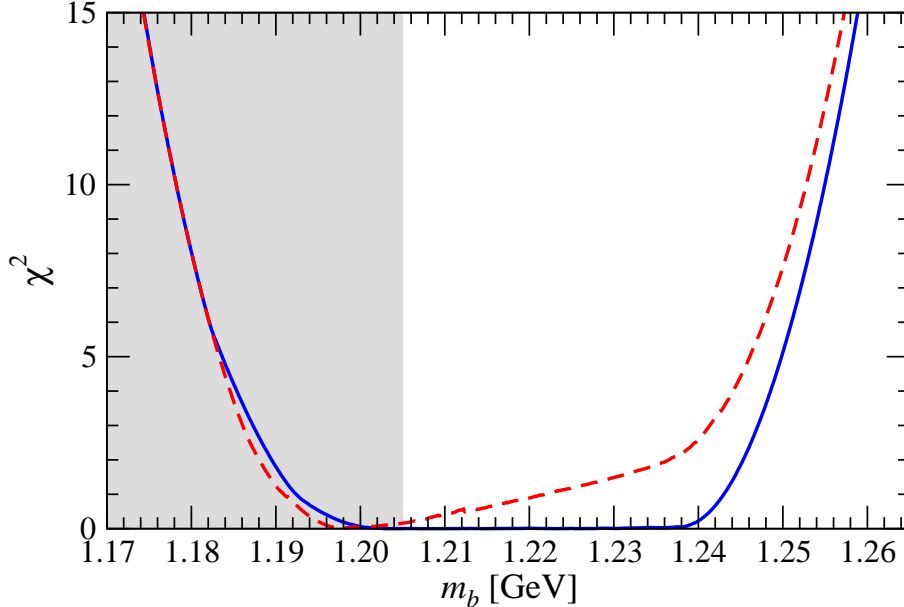


Figure 3:  $\chi^2$  as a function of the bottom-quark mass  $m_b$ . The solid line corresponds to normal neutrino mass ordering, while the dashed line refers to the inverted neutrino mass spectrum. The shaded region indicates the  $1\sigma$  interval for  $m_b$  from Table 1.

In summary, our scenario imposes rather rigid constraints on  $m_b$  and favors  $b - \tau$  unification. This feature is apparently caused by the  $SO(10)$  relation (13) between the mass matrices of charged-leptons and down-quarks, which differ only by a factor of  $-3$  in the off-diagonal matrix elements.

## 5 Conclusions

In this paper we have presented an attempt to combine an  $SO(10)$  GUT with the family symmetry  $A_4$ . We have considered renormalizable Yukawa interactions, therefore, the choice of scalar  $SO(10)$ -plets for fermion mass matrices is confined to  $\mathbf{10}$ ,  $\mathbf{120}$  and  $\overline{\mathbf{126}}$ . The three fermion families are accommodated in an  $A_4$  triplet. For fitting purposes we use the fermion masses at the GUT scale evolved by the renormalization group equations of the MSSM. As a further important prerequisite we assume that the VEVs occurring in the scalar  $SO(10)$  multiplets can be freely chosen for the purpose of fitting fermion masses and mixings. Our investigation consists of two steps—for the details see Section 3.

In the first step we have considered only the down-quark and charged-lepton mass matrices. We have assigned all possible  $A_4$  representations to the  $\mathbf{10}$ ,  $\mathbf{120}$  and  $\overline{\mathbf{126}}$  and checked, if the down-quark and charged-lepton masses can correctly be reproduced. In this way we have identified a unique successful scenario given by the  $\mathbf{10}$  in  $\mathbf{1} \oplus \mathbf{1}' \oplus \mathbf{1}''$  of  $A_4$  and the  $\overline{\mathbf{126}}$  in the  $\mathbf{3}$  of  $A_4$ . This is a non-trivial result, because we use only six masses for probing mass matrices constructed with more than six parameters. The mass matrices (13) of the successful scenario (9) reflect the  $SO(10) \times A_4$  structure: The 10-plets

contribute a general diagonal and the 126-plets a general off-diagonal matrix to the mass matrices.

In the second step we have assumed type II dominance in the seesaw mechanism generating light neutrino masses. Since only the 126-plets contribute to the neutrino mass matrix, we obtain the Zee–Wolfenstein mass matrix.

The scenario gives an excellent fit to all known data on fermion masses and mixings and shows, therefore, the compatibility of the family group  $A_4$  with  $SO(10)$  GUTs. In summary, we have found the following features:

- All mass matrices are symmetric.
- In the charged-fermion sector, as an effect of  $SO(10) \times A_4$ , the building blocks of the mass matrices are general diagonal and off-diagonal matrices, generated by the VEVs of scalar 10-plets and 126-plets, respectively.
- $\mathcal{M}_\nu$  is given by the Zee–Wolfenstein matrix with its definite predictions for the neutrino masses derived from Eq. (2).
- The scenario can equally well accommodate normal and inverted neutrino mass spectra.
- The lepton mixing angles of the Zee–Wolfenstein mass matrix which are in disagreement with the data are corrected by contributions to the PMNS matrix from  $M_\ell$ .
- There are definite predictions for  $|\langle m_{\beta\beta} \rangle|$  for both spectra.
- Our scenario gives  $b$ – $\tau$  Yukawa unification.

On the negative side we note that our scenario does not feature tri-bimaximal lepton mixing, however, some minor constraints on the lepton mixing angles exist—see Sections 4.1 and 4.2. Moreover, up-quark masses and the CKM matrix are completely free and can thus be adapted to the data without imposing any restrictions on the parameters of the mass matrices  $M_d$ ,  $M_\ell$  and  $\mathcal{M}_\nu$ .

**Acknowledgments:** We thank L. Lavoura for valuable suggestions and reading the manuscript.

## References

- [1] H. Fritzsch, P. Minkowski, *Ann. Phys.* 93 (1975) 193.
- [2] P. Minkowski, *Phys. Lett. B* 67 (1977) 421;  
T. Yanagida, in *Proceedings of the Workshop on Unified Theory and Baryon Number in the Universe*, O. Sawata and A. Sugamoto eds., KEK report 79-18, Tsukuba, Japan, 1979;  
S.L. Glashow, in *Quarks and Leptons, Proceedings of the Advanced Study Institute (Cargèse, Corsica, 1979)*, J.-L. Basdevant et al. eds., Plenum, New York, 1981;  
M. Gell-Mann, P. Ramond, and R. Slansky, in *Supergravity*, D.Z. Freedman and F. van Nieuwenhuizen eds., North Holland, Amsterdam, 1979;  
R.N. Mohapatra, G. Senjanović, *Phys. Rev. Lett.* 44 (1980) 912.
- [3] G. Lazarides, Q. Shafi, C. Wetterich, *Nucl. Phys. B* 181 (1981) 287;  
R.N. Mohapatra, G. Senjanović, *Phys. Rev. D* 23 (1981) 165;  
R.N. Mohapatra, P. Pal, *Massive Neutrinos in Physics and Astrophysics*, World Scientific, Singapore, 1991, p. 127.
- [4] J. Schechter, J.W.F. Valle, *Phys. Rev. D* 22 (1980) 2227;  
S.M. Bilenky, J. Hošek, S.T. Petcov, *Phys. Lett. B* 94 (1980) 495;  
I.Yu. Kobzarev, B.V. Martemyanov, L.B. Okun, M.G. Shchepkin, *Yad. Phys.* 32 (1980) 1590 [*Sov. J. Nucl. Phys.* 32 (1981) 823];  
J. Schechter, J.W.F. Valle, *Phys. Rev. D* 25 (1982) 774.
- [5] C.S. Aulakh, R.N. Mohapatra, *Phys. Rev. D* 28 (1983) 217;  
T.E. Clark, T.K. Kuo, N. Nakagawa, *Phys. Lett.* 115B (1982) 26;  
K.S. Babu, R.N. Mohapatra, *Phys. Rev. Lett.* 70 (1993) 2845 [[hep-ph/9209215](#)];  
C.S. Aulakh, B. Bajc, A. Melfo, G. Senjanović, F. Vissani, *Phys. Lett. B* 588 (2004) 196 [[hep-ph/0306242](#)].
- [6] K. Matsuda, Y. Koide, T. Fukuyama, *Phys. Rev. D* 64 (2001) 053015 [[hep-ph/0010026](#)];  
K. Matsuda, Y. Koide, T. Fukuyama, H. Nishiura, *Phys. Rev. D* 65 (2002) 033008 (Err. *ibid.* D 65 (2002) 079904) [[hep-ph/0108202](#)];  
T. Fukuyama, N. Okada, *JHEP* 11 (2002) 011 [[hep-ph/0205066](#)];  
B. Bajc, G. Senjanović, F. Vissani, *Phys. Rev. Lett.* 90 (2003) 051802 [[hep-ph/0210207](#)];  
H.S. Goh, R.N. Mohapatra, S.P. Ng, *Phys. Lett. B* 570 (2003) 215 [[hep-ph/0303055](#)];  
H.S. Goh, R.N. Mohapatra, S.P. Ng, *Phys. Rev. D* 68 (2003) 115008 [[hep-ph/0308197](#)];  
B. Bajc, G. Senjanović, F. Vissani, *Phys. Rev. D* 70 (2004) 093002 [[hep-ph/0402140](#)];  
K.S. Babu, C. Macesanu, *Phys. Rev. D* 72 (2005) 115003 [[hep-ph/0505200](#)].
- [7] S. Bertolini, T. Schwetz, M. Malinský, *Phys. Rev. D* 73 (2006) 115012 [[hep-ph/0605006](#)].



- [8] K. Matsuda, T. Fukuyama, H. Nishiura, Phys. Rev. D 61 (2000) 053001 [hep-ph/9906433];  
S. Bertolini, M. Frigerio, M. Malinský, Phys. Rev. D 70 (2004) 095002 [hep-ph/0406117];  
S. Bertolini, M. Malinský, Phys. Rev. D 72 (2005) 055021 [hep-ph/0504241].
- [9] C.S. Aulakh, hep-ph/0602132;  
W. Grimus, H. Kühböck, Phys. Lett. B 643 (2006) 182 [hep-ph/0607197];  
W. Grimus, H. Kühböck, Eur. Phys. J. C 51 (2007) 721 [hep-ph/0612132];  
C.S. Aulakh, hep-ph/0607252;  
C.S. Aulakh, talk presented at *33rd International Conference on High Energy Physics (ICHEP06)*, Moscow, Russia, July 26–August 2, 2006, hep-ph/0610097;  
C.S. Aulakh, S.K. Garg, hep-ph/0612021.
- [10] C.S. Aulakh, expanded version of the plenary talks at the *Workshop Series on Theoretical High Energy Physics*, IIT Roorkee, Uttaranchal, India, March 16–20, 2005, and at the *8th European Meeting “From the Planck Scale to the Electroweak Scale” (PLANCK05)*, ICTP, Trieste, Italy, May 23–28, 2005, hep-ph/0506291;  
B. Bajc, A. Melfo, G. Senjanović, F. Vissani, Phys. Lett. B 634 (2006) 272 [hep-ph/0511352];  
C.S. Aulakh, S.K. Garg, Nucl. Phys. B 757 (2006) 47 [hep-ph/0512224].
- [11] M. Maltoni, T. Schwetz, M.A. Tórtola, J.W.F. Valle, New. J. Phys. 6 (2004) 122 [hep-ph/0405172];  
G.L. Fogli, E. Lisi, A. Marrone, A. Palazzo, Prog. Part. Nucl. Phys. 57 (2006) 742 [hep-ph/0506083].
- [12] D.G. Lee, R.N. Mohapatra, Phys. Lett. B 329 (1994) 463 [hep-ph/9403201];  
C. Hagedorn, M. Lindner, R.N. Mohapatra, JHEP 0606 (2006) 042 [hep-ph/0602244];  
Yi Cai, Hai-Bo Yu, Phys. Rev. D 74 (2006) 115005 [hep-ph/0608022].
- [13] S. Morisi, M. Picariello, E. Torrente-Lujan, Phys. Rev. D 75 (2007) 075017 [hep-ph/0702034].
- [14] E. Ma, G. Rajasekaran, Phys. Rev. D 64 (2001) 113012 [hep-ph/0106291];  
K.S. Babu, E. Ma, J.W.F. Valle, Phys. Lett. B 552 (2003) 207 [hep-ph/0206292];  
M. Hirsch, E. Ma, A. Villanova del Moral, J.W.F. Valle, Phys. Rev. D 72 (2005) 091301 (Err. *ibid.* D 72 (2005) 119904) [hep-ph/0507148];  
G. Altarelli and F. Feruglio, Nucl.Phys. B 720 (2005) 64 [hep-ph/0504165];  
G. Altarelli and F. Feruglio, Nucl.Phys. B 741 (2005) 215 [hep-ph/0512103];  
E. Ma, Phys. Rev. D 73, 057304 (2006) [hep-ph/0511133];  
E. Ma, H. Sawanaka, M. Tanimoto, Phys. Lett. B 641 (2006) 301 [hep-ph/0606103];  
L. Lavoura, H. Kühböck, Mod. Phys. Lett. A 22 (2007) 181 [hep-ph/0610050];  
and references therein.
- [15] G. Altarelli, Lectures given at the 61st Scottish Universities Summer School in Physics, St. Andrews, Scotland, 8–23 August 2006, hep-ph/0611117.

- [16] P.F. Harrison, D.H. Perkins, W.G. Scott, Phys. Lett. B 530 (2002) 167 [hep-ph/0202074].
- [17] E. Ma, Mod. Phys. Lett. A 21 (2006) 2931 [hep-ph/0607190].
- [18] A. Zee, Phys. Lett. 93B (1980) 389; *ibid.* 161B (1985) 141.
- [19] L. Wolfenstein, Nucl. Phys. B 175 (1980) 93.
- [20] C. Jarlskog, M. Matsuda, S. Skadhauge and M. Tanimoto, Phys. Lett. B 449 (1999) 240 [hep-ph/9812282];  
P.H. Frampton and S.L. Glashow, Phys. Lett. B 461 (1999) 95 [hep-ph/9906375].
- [21] W. Konetschny and W. Kummer, Phys Lett. 70B (1977) 433;  
T.P. Cheng and L.-F. Lee, Phys. Rev. D22 (1980) 2860.
- [22] Xiao-Gang He and A. Zee, Phys. Rev. D 68 (2003) 037302 [hep-ph/0302201].
- [23] T. Schwetz, Phys. Scripta T 127 (2006) 1 [hep-ph/0606060].
- [24] K.R.S. Balaji, W. Grimus, T. Schwetz, Phys. Lett. B 508 (2001) 301 [hep-ph/0104035];  
Y. Koide, Phys. Rev. D 64 (2001) 077301 [hep-ph/0104226].
- [25] C. Giunti, M. Tanimoto, Phys.Rev. D 66 (2002) 053013 [hep-ph/0207096];  
C. Giunti, M. Tanimoto, Phys. Rev. D 66 (2002) 113006 [hep-ph/0209169];  
P.H. Frampton, S.T. Petcov, W. Rodejohann, Nucl. Phys. B687 (2004) 31 [hep-ph/0401206];  
K.A. Hochmuth, S.T. Petcov, W. Rodejohann, arXiv:0706.2975.
- [26] R.N. Mohapatra, B. Sakita, Phys. Rev. D 21 (1980) 1062.
- [27] R. Slansky, Phys. Rept. 79 (1981) 1.
- [28] J.A. Nelder, R. Mead, Comp. J. 7 (1965) 306;  
W.H. Press, B.P. Flannery, S.A. Teukolsky, W.T. Vetterling, *Numerical recipes in C: The art of scientific computing*, Cambridge University Press, 1992.
- [29] S. Dimopoulos, F. Wilczek, in: *The Unity of the Fundamental Interactions*, Proceedings of the 19th Course of the International School of Subnuclear Physics, Erice, Italy, 1981, edited by A. Zichini (Plenum Press, New York, 1983) 237-249;  
K.S. Babu, S.M. Barr, Phys. Rev. D 48 (1993) 5354 [hep-ph/9306242].
- [30] K.S. Babu, I. Gogoladze, Z. Tavartkiladze, Phys. Lett. B 650 (2007) 49 [hep-ph/0612315].
- [31] C.S. Aulakh, A. Girdar, Int. J. Mod. Phys. A 20 (2005) 865 [hep-ph/0204097];  
B. Bajc, A. Melfo, G. Senjanović, F. Vissani, Phys. Rev. D 70 (2004) 035007 [hep-ph/0402122].

- [32] C.R. Das, M.K. Parida, Eur. Phys. J. C 20 (2001) 121 [hep-ph/0010004].
- [33] W.-M. Yao et al., *Review of Particle Physics*, J. Phys. G 33 (2006) 1.
- [34] S. Antusch, J. Kersten, M. Lindner, M. Ratz, Nucl. Phys. B 674 (2003) 401 [hep-ph/0305273].
- [35] See for instance  
S. Hannestad and G. Raffelt, JCAP 04 (2004) 008 [hep-ph/0312154];  
Ø. Elgarøy and O. Lahav, New J. Phys. 7 (2005) 61 [hep-ph/0412075];  
A. Goobar, S. Hannestad, E. Mörtzell and H. Tu, JCAP 06 (2006) 019 [astro-ph/0602155];  
M. Fukugita, K. Ichikawa, M. Kawasaki and O. Lahav, Phys. Rev. D 74 (2006) 027302 [astro-ph/0605362];  
and references therein.